Article

Not peer-reviewed version

Quark Deconfinement Phase Transition in Hot Neutron-Star Matter: Effects of Neutrino Trapping

Grigor Alaverdyan * and Ani Alaverdyan

Posted Date: 9 March 2026

doi: 10.20944/preprints202603.0555.v1

Keywords: quark matter; NJL model; hadronic matter; RMF model; hot; deconfinement; trapped neutrinos; critical endpoint

 doi:10.20944/preprints202603.0555.v1

Article

Quark Deconfinement Phase Transition in Hot Neutron-Star Matter: Effects of Neutrino Trapping

Grigor Alaverdyan * **and Ani Alaverdyan**

Yerevan State University, 1 Alex Manoogian Street, Yerevan 0025, Armenia
* Correspondence: galaverdyan@ysu.am

Abstract

We study the effect of trapped neutrinos on the properties of the deconfinement phase transition from hot β-equilibrated, electrically neutral hadronic matter to quark matter. To describe the thermodynamic properties of hot hadronic matter, an extended relativistic mean field (RMF) theory is used, which also incorporates the isovector–Lorentz-scalar δ-meson effective field. The three-flavor quark phase is described within the framework of the local Nambu–Jona-Lasinio (NJL) model. It was assumed that the surface tension at the quark-hadron interface is so strong that the phase transition occurs according to Maxwell's construction. The thermodynamic properties of the quark and hadronic phases were calculated for both neutrino-trapped and neutrino-transparent regimes at various temperatures ranging from 0 to 100 MeV and baryon number densities from 0 to 1.8 fm^{-3}. The impact of trapped neutrinos on the thermodynamic properties of the coexistence state has been investigated. It has been demonstrated that the baryon chemical potential in the coexistence state decreases as temperature increases. The critical endpoint parameters in the $T - n_B$ plane of the phase diagram were obtained for the case of trapped neutrinos (74 MeV; 0.269 fm^{-3}) and for the case of the absence of neutrinos (75.6 MeV; 0.255 fm^{-3}).

Keywords: quark matter; NJL model; hadronic matter; RMF model; hot; deconfinement; trapped neutrinos; critical endpoint

---

1. Introduction

The investigation of the structure, constituent composition, and thermodynamic properties of strongly interacting superdense matter is one of the fundamental problems in modern nuclear physics, particle physics, and astrophysics. Quantum chromodynamics (QCD) predicts that at extremely high temperatures and/or densities, a quark–gluon plasma (QGP) consisting of deconfined quarks and gluons is formed [1,2].

The only currently available opportunity to obtain information about the formation and properties of quark matter in terrestrial laboratory conditions is through heavy ion collisions. During heavy-ion collisions, when hundreds of nucleons hit each other, conditions arise for the formation of short-lived states in which quarks are deconfined and a QGP is formed. Analyzing the final particles produced from collisions, along with the various patterns observed in this process, enables researchers to identify the formation of the QGP. This analysis, combined with modern theoretical insights, allows for the study of the properties of QGP and the QCD processes that contribute to its formation and evolution (see e.g. [3–8]).

Review articles [9,10] provides a thorough overview of the current understanding of QGP formed in high-energy collisions. It explores the properties of this state of matter, key experimental observables, and the theoretical framework that describes it. Another way to determine the existence of quark matter and learn about its properties is to study cosmic-scale bodies, such as compact stars, whose central density is so high that conditions are created for the formation of quark matter [11–14].

 doi:10.20944/preprints202603.0555.v1

The properties of compact stars depend on the equation of state of matter across a wide density range, from ordinary atomic matter to densities much higher than nuclear density. At these extreme levels, exotic phases can emerge, such as pion and kaon condensates, deconfined quark phases, and color superconducting phases.

Theoretical studies of macroscopic parameters of compact stars help refine the equation of state of superdense matter by comparing them with observational data and ruling out conflicting models. This approach to refining the equation of state has been made more efficient by the Neutron Star Interior Composition Explorer (NICER) astrophysics mission, which has allowed it to simultaneously determine the mass and radius of the same pulsar [15–17].

In the last few decades, the equations of state of cold hadronic matter and quark matter have been intensively discussed, both separately and in hybrid cases involving phase transitions. In a significant number of works, a phenomenological model, such as the MIT quark bag model [18], has been chosen to describe the quark phase (see e.g.,[19–27]). Using the equation of state of cold matter, the observable global characteristics of hybrid stars have been calculated. Such equations of state clearly do not apply to heavy ion collisions, the core collapse of supernovae, proto-neutron stars, or the merger of binary compact stars, since the temperatures in these cases are quite high. In the post-merger phase, temperatures are expected to reach as high as approximately 50 to 100 MeV, making it suitable for studies at finite temperatures [28].

The equation of state of hot quark matter within the framework of the MIT–bag model was studied in Refs. [29–34]. Given that the matter of a neutron star at high temperatures is not transparent to neutrinos, in these works, in addition to quarks, electrons, and muons, the presence of various neutrino types was also taken into account.

Recently, the Nambu–Jona-Lasinio (NJL) model [35,36] has been frequently used to describe quark matter. It is well known that the NJL model successfully reproduces many features of QCD [37–39]. Within the framework of the NJL model, the equation of state of quark matter was studied and applied to calculate the structure and observable global parameters of hybrid stars with quark cores [40–45].

In this work, we investigate the effect of trapped neutrinos on the properties of the deconfinement phase transition from hot β-equilibrated, electrically neutral hadronic matter to three-flavor quark matter. The thermodynamic description of hot hadronic matter was carried out within the framework of the relativistic mean-field (RMF) theory [46,47], in which, along with other meson fields, the isovector–Lorentz-scalar δ-meson field was also taken into account [24,48,49].

Hot quark matter was analyzed using the NJL SU(3) local model [35,36]. The thermodynamic properties were evaluated in two scenarios: one where neutrinos are trapped within the system, and another where the neutrinos produced by β-decays have already escaped [50]. For the phase transition from hadronic matter to quark matter, Maxwell's construction was used, which is based on the condition of local electric neutrality.

The paper is organized as follows: In Section 2, we outline the theoretical framework for the thermodynamic description of strongly interacting hot matter. This section is divided into three Subsections. In subsection 2.1 we present the thermodynamic description of beta-equilibrium hot quark matter under neutrino trapping conditions within the framework of the three-flavor local NJL model. In Section 2.2, we present the thermodynamic description of hot hadronic matter under neutrino trapping conditions within the framework of RMF theory. Subsection 2.3 is devoted to determining the characteristics of the first-order phase transition from hadronic matter to quark matter at finite temperatures based on Maxwell's construction. The graphical and tabular results of the numerical calculations, along with their discussion, are presented in Section 3, and conclusions are drawn in Section 4.

 doi:10.20944/preprints202603.0555.v1

2. Theoretical Framework

2.1. Neutrino-Trapped Quark Matter Within the Local SU(3) NJL Model

For the thermodynamic description of quark matter, we will utilize the local SU(3) model developed by Nambu–Iona-Lasinio[35,36]. Our focus will be on a multiparticle system that consists of up (u), down (d), and strange (s) quarks, electrons (e^-), electron neutrinos (ν_e), muons (μ^-), muon neutrinos (ν_μ), as well as their corresponding antiparticles. We overlook the τ-leptons, assuming they are too heavy to be produced in a medium.

The Lagrangian density of the system will be represented in the form of two summands, the first of which will describe the quark component, and the second the lepton part:

$$\mathcal{L}_{QM} = \mathcal{L}_{NJL} + \mathcal{L}_{Lept}, \tag{1}$$

The Lagrangian density of the quark component in terms of the SU(3) NJL model is given by

$$\begin{aligned}\mathcal{L}_{NJL} = \overline{\psi}(i\gamma^\mu\partial_\mu - \hat{m}_0)\psi + G\sum_{a=0}^{8}\Big[(\overline{\psi}\lambda_a\psi)^2 + (\overline{\psi}i\gamma_5\lambda_a\psi)^2\Big] \\ -K\Big\{det_f\big(\overline{\psi}(1+\gamma_5)\psi\big) + det_f\big(\overline{\psi}(1-\gamma_5)\psi\big)\Big\}.\end{aligned} \tag{2}$$

Here ψ is the Fermion quark spinor field ${\psi_f}^c$c with three flavors $f = u,\ d,\ s$ and three colors $c = r\ ,g,\ b$. The first term is the density of the Dirac Lagrangian of free quark fields with a mass matrix of current quarks $\hat{m}_0 = \text{diag}\ (m_{0u},\ m_{0d},\ m_{0s})$. The second corresponds to a chirally-symmetric four-quark interaction with a coupling constant G, where λ_a $(a = 1, 2, ..., 8)$ are the Gell-Mann matrices and generators of the SU(3) group in flavor space, $\lambda_0 = \sqrt{2/3}\hat{I}$ ($\hat{I}$ is the unit 3 ×3 matrix). The third term corresponds to the six-quark Kobayashi-Maskawa-'t Hooft interaction, which breaks the axial $U_A(1)$ symmetry.

For the leptonic component, we used the Lagrangian density of free particles,

$$\mathcal{L}_{Lept} = \sum_{l=e,\nu_e,\mu,\nu_\mu} \overline{\psi}_l(i\gamma^\mu\partial_\mu - m_l)\,\psi_l, \tag{3}$$

where $m_e = 0.511$ MeV and $m_\mu = 105.6$ MeV are the masses of the electrons and muons, respectively. We assumed that neutrinos are massless particles.

The NJL model is an effective, nonrenormalizable model, so a cut-off Λ is implemented in 3-momentum space to regularize divergent integrals.

Based on the expression for the Lagrangian density (1), we can derive a formula for the grand canonical potential $\Omega_{NJL}(T, \{M_f\}, \{\mu_f\})$ of the quark component, which is determined up to an additive constant. Assuming that in the case of a vacuum, the grand canonical potential is equal to zero, for a quark matter, we can write [1]

[1] We use the natural system of units with $\hbar = k_B = c = 1$.

 doi:10.20944/preprints202603.0555.v1

$$
\begin{aligned}
\Omega_{QM}(T,\{M_f\},\{\mu_f\},\{\mu_l\}) = -\frac{3}{\pi^2}\sum_{f=u,d,s}\left\{\int_0^{\Lambda} dk\, k^2\Big(E(k,M_f)-E(k,M_{f0})\Big)\right\} \\
-\frac{3T}{\pi^2}\sum_{f=u,d,s}\left\{\int_0^{\Lambda} dk\, k^2\Big[ln\Big(1+e^{-\left(E(k,M_f)-\mu_f\right)/T}\Big)+ln\Big(1+e^{-\left(E(k,M_f)+\mu_f\right)/T}\Big)\Big]\right\} \\
+2G\sum_{f=u,d,s}\sigma_f(T,M_f,\mu_f)^2-4K\sigma_u(T,M_u,\mu_u)\,\sigma_d(T,M_d,\mu_d)\,\sigma_s(T,M_s,\mu_s) \\
-2G\sum_{f=u,d,s}{\sigma_{f0}}^2+4K\sigma_{u0}\,\sigma_{d0}\,\sigma_{s0} \\
-\frac{T}{\pi^2}\sum_{l=e,\mu}\left\{\int_0^{\infty} dk\, k^2\Big[ln\Big(1+e^{-(E(k,m_l)-\mu_l)/T}\Big)+ln\Big(1+e^{-(E(k,m_l)+\mu_l)/T}\Big)\Big]\right\} \\
-\frac{1}{2\pi^2}T\sum_{l=\nu_e,\nu_\mu}\left\{\int_0^{\infty} dk\, k^2\Big[ln\Big(1+e^{-(k-\mu_l)/T}\Big)+ln\Big(1+e^{-(k+\mu_l)/T}\Big)\Big]\right\}.
\end{aligned}
\tag{4}
$$

Here, M_f represents the constituent quark mass of flavor f, while M_{f0} represents the constituent quark mass in vacuum, also known as the dressed mass. Similarly, $\sigma_f(T,M_f,\mu_f)=\langle\overline{\psi_f}\psi_f\rangle$ represents the quark condensate, whereas σ_{f0} refers to the same quantity in a vacuum. Additionally, $E(k,M_f)=\sqrt{k^2+{M_f}^2}$ provides the energy of the quark quasiparticle with momentum k, while μ_f stands for the chemical potential. Similarly, $E(k,m_l)=\sqrt{k^2+{m_l}^2}$ and μ_l represent the energy and chemical potential of a lepton, respectively.

In the mean-field approximation, the gap equations for the constituent masses of the quarks M_u, M_d, and M_s are given by

$$
\begin{aligned}
M_u &= m_{0u}-4\,G_S\,\sigma_u+2\,K\sigma_d\,\sigma_s, \\
M_d &= m_{0d}-4\,G_S\,\sigma_d+2\,K\sigma_s\,\sigma_u, \\
M_s &= m_{0s}-4\,G_S\,\sigma_s+2\,K\sigma_u\,\sigma_d.
\end{aligned}
\tag{5}
$$

The equations for quark condensates $\sigma_f(T,M_f,\mu_f)$, $f=u,\ d,\ s$ are written as follows:

$$
\sigma_f = -\frac{3M_f}{\pi^2}\int_0^{\Lambda} dk\,\frac{k^2}{E(k,M_f)}\left[1-\frac{1}{1+e^{\left(E(k,M_f)-\mu_f\right)/T}}-\frac{1}{1+e^{\left(E(k,M_f)+\mu_f\right)/T}}\right].
\tag{6}
$$

The quark number densities are determined by the expression

$$
n_f(T,M_f,\mu_f)=\frac{3}{\pi^2}\int_0^{\Lambda} dk\, k^2\left[\Big(1+e^{\left(E(k,M_f)-\mu_f\right)/T}\Big)^{-1}-\Big(1+e^{\left(E(k,M_f)+\mu_f\right)/T}\Big)^{-1}\right].
\tag{7}
$$

The lepton number densities are calculated using the following formula:

$$
n_l(T,m_l,\mu_l)=\frac{1}{2\pi^2}g_l\int_0^{\infty} dk\, k^2\left[\Big(1+e^{(E_l(k,m_l)-\mu_l)/T}\Big)^{-1}-\Big(1+e^{(E_l(k,m_l)+\mu_l)/T}\Big)^{-1}\right],
\tag{8}
$$

where $l=e,\nu_e,\mu,\nu_\mu$, and g_l is the lepton degeneracy factor, whose values are: $g_e=g_\mu=2$; $g_{\nu_e}=g_{\nu_\mu}=1$.

For the electrical neutrality condition of quark matter, we have

$$
\frac{2}{3}n_u-\frac{1}{3}n_d-\frac{1}{3}n_s-n_e-n_\mu=0.
\tag{9}
$$

In this work, we have ignored neutrino oscillation effects and assumed that the lepton number for different lepton flavors is separately conserved. Let us denote the fraction of the electron lepton number (the electron lepton number per baryon) by Y_{L_e}, and the fraction of the muon lepton number by Y_{L_μ}.

The relationship between lepton concentrations will be written as

$$n_e + n_{\nu_e} = Y_{L_e}\, n_B, \tag{10}$$

$$n_\mu + n_{\nu_\mu} = Y_{L_\mu}\, n_B. \tag{11}$$

When trapped neutrinos are introduced into the model, additional parameters appear, such as the chemical potentials of neutrinos: μ_{ν_e} and μ_{ν_μ}. It becomes necessary to have two new known characteristics. As such characteristics, we have chosen the lepton fractions, assuming that they are constant and equal: $Y_{L_e} = 0.4$, $Y_{L_\mu} = 0$ [51–54].

For quark matter in β-equilibrium, the following conditions will be satisfied for the chemical potentials of the particles:

$$\mu_d = \mu_s = \mu_u + \mu_e - \mu_{\nu_e} = \mu_u + \mu_\mu - \mu_{\nu_\mu}. \tag{12}$$

The baryon number density is expressed in terms of quark densities as follows:

$$n_B = \frac{1}{3}(n_u + n_d + n_s). \tag{13}$$

For a given baryon number density n_B and temperature T, by numerically solving the system of 20 equations (5)–(13), we will find the 20 unknown characteristics for the electrically neutral quark matter in β-equilibrium: $\{M_f\}$, $\{\sigma_f\}$, $\{n_i\}$, and $\{\mu_i\}$ ($f = u, d, s;\ i = u, d, s, e, \nu_e, \mu, \nu_\mu$).

Knowledge of these characteristics makes it possible, for specified values of the baryon number density n_B and temperature T, to determine the other key thermodynamic parameters of electrically neutral β-equilibrium quark matter, such as pressure, energy density, and entropy density.

The pressure of quark matter with neutrino trapping is determined by the following expression:

$$\begin{aligned} P_{QM} = {}& \frac{3}{\pi^2}\sum_{f=u,d,s}\left\{\int_0^\Lambda dk\, k^2\left[E_f(k,M_f) - E_f(k,M_{f0})\right]\right\} \\ &+\frac{3T}{\pi^2}\sum_{f=u,d,s}\left\{\int_0^\Lambda dk\, k^2\left[ln\left(1+e^{-(E_f(k,M_f)-\mu_f)/T}\right) + ln\left(1+e^{-(E_f(k,M_f)+\mu_f)/T}\right)\right]\right\} \\ &-2G(\sigma_u^2+\sigma_d^2+\sigma_s^2-\sigma_{u0}^2-\sigma_{d0}^2-\sigma_{s0}^2) + 4K(\sigma_u\,\sigma_d\,\sigma_s - \sigma_{u0}\,\sigma_{d0}\,\sigma_{s0}) \\ &+\frac{T}{2\pi^2}\sum_{l=e,\mu,\nu_e,\nu_\mu}\left\{g_l\int_0^\infty dk\, k^2\left[ln\left(1+e^{-(E_l(k,m_l)-\mu_l)/T}\right) + ln\left(1+e^{-(E_l(k,m_l)+\mu_l)/T}\right)\right]\right\}. \end{aligned} \tag{14}$$

The expression for the energy density of quark matter with neutrino trapping has the form

$$\begin{aligned} \varepsilon_{QM} = {}& \frac{3}{\pi^2}\sum_{f=u,d,s}\left\{\int_0^\Lambda dk\, k^2\left[E_f(k,M_{f0}) - E_f(k,M_f)\right]\right\} \\ &+\frac{3}{\pi^2}\sum_{f=u,d,s}\left\{\int_0^\Lambda dk\, k^2 E_f(k,M_f)\left[\left(1+e^{(E_f(k,M_f)-\mu_f)/T}\right)^{-1} + \left(1+e^{(E_f(k,M_f)+\mu_f)/T}\right)^{-1}\right]\right\} \\ &+2G(\sigma_u^2+\sigma_d^2+\sigma_s^2-\sigma_{u0}^2-\sigma_{d0}^2-\sigma_{s0}^2) - 4K(\sigma_u\,\sigma_d\,\sigma_s - \sigma_{u0}\,\sigma_{d0}\,\sigma_{s0}) \\ &+\frac{1}{2\pi^2}\sum_{l=e,\mu,\nu_e,\nu_\mu}\left\{g_l\int_0^\infty dk\, k^2 E_l(k,m_l)\left[\left(1+e^{(E_l(k,m_l)-\mu_l)/T}\right)^{-1} + \left(1+e^{(E_l(k,m_l)+\mu_l)/T}\right)^{-1}\right]\right\} \end{aligned} \tag{15}$$

The entropy density of quark matter with neutrino trapping is given by

 doi:10.20944/preprints202603.0555.v1

$$
\begin{aligned}
S_{QM} = \frac{3}{\pi^2} \sum_{f=u,d,s} \Bigg\{ \int_0^{\Lambda} dk\, k^2 \Big[ln\Big(1+e^{-(E(k,M_f)-\mu_f)/T}\Big) + ln\Big(1+e^{-(E(k,M_f)+\mu_f)/T}\Big)\Big]\Bigg\} \\
+\frac{3}{\pi^2 T} \sum_{f=u,d,s} \Bigg\{ \int_0^{\Lambda} dk\, k^2 E(k,M_f) \Big[\Big(1+e^{(E(k,M_f)-\mu_f)/T}\Big)^{-1} + \Big(1+e^{(E(k,M_f)+\mu_f)/T}\Big)^{-1}\Big]\Bigg\} \\
+\frac{1}{2\pi^2} \sum_{f=e,\mu,\nu_e,\nu_\mu} g_l \Bigg\{ \int_0^{\infty} dk\, k^2 \Big[ln\Big(1+e^{-(E(k,m_l)-\mu_l)/T}\Big) + ln\Big(1+e^{-(E(k,m_l)+\mu_l)/T}\Big)\Big]\Bigg\} \\
-\frac{1}{T} \sum_{f=u,d,s} \mu_f n_f - \frac{1}{T} \sum_{l=e,\mu,\nu_e,\nu_\mu} \mu_l n_l. \qquad (16)
\end{aligned}
$$

The parameters used to calculate the thermodynamic characteristics of three-flavor quark matter are as follows: $\Lambda = 602.3$ MeV, $G = 1.835/\Lambda^2$ and $K = 12.36/\Lambda^5$, $m_{0u} = m_{0d} = 5.5$ MeV, $m_{0s} = 140.7$ MeV obtained in Ref. [37], for reproducing the values of the coupling constant of the pion, $f_\pi = 92.4$ MeV, as well as the masses of the π, K, η and η' mesons, $m_\pi = 135$ MeV, $m_K = 497.7$ MeV, $m_\eta = 514.8$ MeV, and $m_{\eta'} = 960.8$ MeV, respectively.

2.2. Neutrino-Trapped Hadronic Matter Within the RMF Model

For the thermodynamic description of beta-equilibrium hadronic matter consisting of neutrons (n), protons (p), electrons (e), electron neutrinos (ν_e), muons (μ), and muon neutrinos (ν_μ), we will use the relativistic mean field (RMF) approach within the framework of quantum hadrodynamics (QHD) [46,47]. In this theory, the strong interaction between nucleons is mediated by the exchange of mesons. The exchanged mesons include the isoscalar-Lorentz-scalar meson σ; the isoscalar-Lorentz-vector meson ω; the isovector-Lorentz-scalar meson δ; and the isovector-Lorentz-vector meson ρ. The relativistic nonlinear Lagrangian density for hadronic matter of this composition is expressed as follows:

$$
\mathcal{L}_{HM} = \mathcal{L}_{RMF} + \mathcal{L}_{Lept}, \qquad (17)
$$

As in the case of quark matter, here we will also ignore the interaction between leptons and use equation (3) for the Lagrangian density of the leptonic component.

The Lagrangian density for the hadronic component within the nonlinear RMF model is given by

$$
\begin{aligned}
\mathcal{L}_{RMF} = \overline{\psi}_N \gamma^\mu \Big(i\partial_\mu - g_\omega \omega_\mu(x) - \frac{1}{2} g_\rho \boldsymbol{\tau}_N \boldsymbol{\rho}_\mu(x) \Big) \psi_N \\
-\overline{\psi}_N (m_N - g_\sigma \sigma(x) - g_\delta \boldsymbol{\tau}_N \boldsymbol{\delta}(x)) \psi_N \\
+\frac{1}{2}\Big(\partial_\mu \sigma(x) \partial^\mu \sigma(x) - m_\sigma \sigma(x)^2\Big) - \frac{b}{3} m_N (g_\sigma \sigma(x))^3 - \frac{c}{4} (g_\sigma \sigma(x))^4 \\
+\frac{1}{2} m_\omega^2 \omega^\mu(x) \omega_\mu(x) - \frac{1}{4} \Omega_{\mu\nu}(x) \Omega^{\mu\nu}(x) \\
+\frac{1}{2}\Big(\partial_\mu \boldsymbol{\delta}(x) \partial^\mu \boldsymbol{\delta}(x) - m_\delta^2 \boldsymbol{\delta}(x)^2\Big) \\
+\frac{1}{2} m_\rho^2 \boldsymbol{\rho}^\mu(x) \boldsymbol{\rho}_\mu(x) - \frac{1}{4} \Re_{\mu\nu}(x) \Re^{\mu\nu}(x) \qquad (18)
\end{aligned}
$$

Here $\psi_N = \begin{pmatrix} \psi_p \\ \psi_n \end{pmatrix}$ is isospin doublet of nucleon bispinors, $\boldsymbol{\tau}_N$ are 2×2 Pauli isospin matrices, $\sigma(x)$, $\omega_\mu(x)$, $\boldsymbol{\delta}(x)$, $\boldsymbol{\rho}_\mu(x)$ are exchange meson fields at space-time point $x = x_\mu = (t,x,y,z)$, m_N, m_e, m_σ, m_ω, m_δ, m_ρ are the masses of the free particles, $\Omega_{\mu\nu}(x)$ and $\Re_{\mu\nu}(x)$ are antisymmetric tensors of the vector fields $\omega_\mu(x)$ and $\boldsymbol{\rho}_\mu(x)$. Additionally, g_σ, g_ω, g_δ, g_ρ denote the coupling constants of the strong interaction between nucleons and corresponding mesons.

In the mean-field approach, the meson fields $\sigma(x)$, $\omega_\mu(x)$, $\boldsymbol{\delta}(x)$, and $\boldsymbol{\rho}_\mu(x)$ are replaced by the (effective) fields $\overline{\sigma}$, $\overline{\omega}_\mu$, $\overline{\boldsymbol{\delta}}$, and $\overline{\boldsymbol{\rho}}_\mu$, respectively. A convenient redefinition of the meson mean-fields and coupling constants

$$g_\sigma \overline{\sigma} = \sigma, \quad g_\omega \overline{\omega}_0 = \omega, \quad g_\delta \overline{\delta}^{(3)} = \delta, \quad g_\rho \overline{\rho}_0^{(3)} = \rho, \tag{19}$$

$$(g_\sigma/m_\sigma)^2 = a_\sigma, \quad (g_\omega/m_\omega)^2 = a_\omega, \quad (g_\delta/m_\delta)^2 = a_\delta, \quad (g_\rho/m_\rho)^2 = a_\rho, \tag{20}$$

allows us to eliminate the meson masses in the Euler-Lagrange equations for meson mean-fields:

$$\sigma = a_\sigma \left(n_{sn} + n_{sp} - b\,\sigma^2 - c\,\sigma^3 \right) \tag{21}$$

$$\omega = a_\omega \left(n_n + n_p \right) \tag{22}$$

$$\delta = -a_\delta \left(n_{sn} - n_{sp} \right) \tag{23}$$

$$\rho = -\frac{1}{2} a_\rho \left(n_n - n_p \right) \tag{24}$$

Nucleon number densities are determined as follows:

$$n_i = \frac{1}{\pi^2} \int\limits_0^\infty dk\, k^2 (f(k, m_i^*, \mu_i^*) - f_a(k, m_i^*, \mu_i^*)), \quad i = p, n. \tag{25}$$

where $m_n^* = m_N - \sigma + \delta$ and $m_p^* = m_N - \sigma - \delta$ are the effective masses of nucleon, and $\mu_n^* = \mu_n - \omega + \frac{1}{2}\rho$ and $\mu_p^* = \mu_p - \omega - \frac{1}{2}\rho$ are the effective chemical potentials for nucleons.

The functions $f(k, m, \mu)$ and $f_a(k, m, \mu)$ are the Fermi–Dirac distribution functions of particles and antiparticles, which are defined as:

$$f(k, m, \mu) = \left(1 + e^{(E(k,m) - \mu)/T} \right)^{-1}, \quad f_a(k, m, \mu) = \left(1 + e^{(E(k,m) + \mu)/T} \right)^{-1}. \tag{26}$$

In the field equations (21) and (23) for the Lorentz-scalar σ and δ mesons, the quantities n_{sn} and n_{sp} represent the scalar number densities of nucleons, which are determined as follows:

$$n_{si} = \frac{1}{\pi^2} \int\limits_0^\infty dk\, k^2 \frac{m_i^*}{E(k, m_i^*)} (f(k, m_i^*, \mu_i^*) - f_a(k, m_i^*, \mu_i^*)), \quad i = p, n. \tag{27}$$

The lepton number density in the hadronic phase is determined by the same formula as in the quark phase (see (8)):

$$n_l(T, m_l, \mu_l) = \frac{1}{2\pi^2} g_l \int_0^\infty dk\, k^2 \left[\left(1 + e^{(E_l(k,m_l) - \mu_l)/T} \right)^{-1} - \left(1 + e^{(E_l(k,m_l) + \mu_l)/T} \right)^{-1} \right], \tag{28}$$

where $l = e, \nu_e, \mu, \nu_\mu$, and g_l is the lepton degeneracy factor, whose values are: $g_e = g_\mu = 2$; $g_{\nu_e} = g_{\nu_\mu} = 1$.

In this case, the condition of electrical neutrality will be

$$n_p - n_e - n_\mu = 0. \tag{29}$$

Equations (10) and (11) written for the fractions of electron and muon lepton numbers Y_e, and Y_μ will also remain valid in the case of hadronic matter.

For hadronic matter in β-equilibrium, the following conditions will be satisfied for the chemical potentials of the particles:

$$\mu_n = \mu_p + \mu_e - \mu_{\nu_e} = \mu_p + \mu_\mu - \mu_{\nu_\mu}. \tag{30}$$

The baryon number density is expressed in terms of nucleon densities as follows:

$$n_B = n_n + n_p. \tag{31}$$

The system of equations (10), (11), (21) –(24), and (29)–(31) for a given value of baryon number density n_B and temperature T is a closed set of ten equations, the numerical solution of which makes it possible to find the meson mean-fields σ, ω, δ, ρ, as well as the chemical potentials of the particles μ_n, μ_p, μ_e, μ_{ν_e}, μ_μ, and μ_{ν_μ}. Knowledge of these quantities allows us to determine the remaining thermodynamic characteristics of beta-equilibrium hadronic matter under neutrino-trapped conditions.

The pressure of hadronic matter in a neutrino trapping regime is determined by the following expression:

$$\begin{aligned} P_{HM} = \frac{1}{3\pi^2} \sum_{i=n,p} \left\{ \int_0^\infty dk \, \frac{k^4}{E(k, m_i^*)} \left(f(k, m_i^*, \mu_i^*) + f_a(k, m_i^*, \mu_i^*) \right) \right\} \\ - \frac{b}{3} m_N \sigma^3 - \frac{c}{4}\sigma^4 + \frac{1}{2}\left(-\frac{\sigma^2}{a_\sigma} + \frac{\omega^2}{a_\omega} - \frac{\delta^2}{a_\delta} + \frac{\rho^2}{a_\rho} \right) \\ + \frac{1}{6\pi^2} \sum_{l=e,\mu,\nu_e,\nu_\mu} \left\{ g_l \int_0^\infty dk \, \frac{k^4}{E(k, m_l)} \left(f(k, m_l, \mu_l) + f_a(k, m_l, \mu_l) \right) \right\}. \end{aligned} \quad (32)$$

The expression for the energy density of hadronic matter in a neutrino trapping regime is given by the following form:

$$\begin{aligned} \varepsilon_{HM} = \frac{1}{\pi^2} \sum_{i=n,p} \left\{ \int_0^\infty dk \, k^2 E(k, m_i^*) \left(f(k, m_i^*, \mu_i^*) + f_a(k, m_i^*, \mu_i^*) \right) \right\} \\ + \frac{b}{3} m_N \sigma^3 + \frac{c}{4}\sigma^4 + \frac{1}{2}\left(\frac{\sigma^2}{a_\sigma} + \frac{\omega^2}{a_\omega} + \frac{\delta^2}{a_\delta} + \frac{\rho^2}{a_\rho} \right) \\ + \frac{1}{2\pi^2} \sum_{l=e,\mu,\nu_e,\nu_\mu} \left\{ g_l \int_0^\infty dk \, k^2 E(k, m_l) \left(f(k, m_l, \mu_l) + f_a(k, m_l, \mu_l) \right) \right\}. \end{aligned} \quad (33)$$

The entropy density of hadronic matter under a neutrino trapping regime is expressed as follows:

$$\begin{aligned} S_{HM} = -\frac{1}{\pi^2} \sum_{i=n,p} \int_0^\infty dk \, k^2 \left(f(k, m_i^*, \mu_i^*) \ln f(k, m_i^*, \mu_i^*) \right) \\ - \frac{1}{\pi^2} \sum_{i=n,p} \int_0^\infty dk \, k^2 \left(fa(k, m_i^*, \mu_i^*) \ln f_a(k, m_i^*, \mu_i^*) \right) \\ - \frac{1}{\pi^2} \sum_{i=n,p} \int_0^\infty dk \, k^2 \left((1 - f(k, m_i^*, \mu_i^*)) \ln(1 - f(k, m_i^*, \mu_i^*)) \right) \\ - \frac{1}{\pi^2} \sum_{i=n,p} \int_0^\infty dk \, k^2 \left((1 - f_a(k, m_i^*, \mu_i^*)) \ln(1 - fa(k, m_i^*, \mu_i^*)) \right) \\ - \frac{1}{2\pi^2} \sum_{l=e,\mu,\nu_e,\nu_\mu} g_l \int_0^\infty dk \, k^2 \left(f(k, m_l, \mu_l) \ln f(k, m_l, \mu_l) \right) \\ - \frac{1}{2\pi^2} \sum_{l=e,\mu,\nu_e,\nu_\mu} g_l \int_0^\infty dk \, k^2 \left(f_a(k, m_l, \mu_l) \ln f_a(k, m_l, \mu_l) \right) \\ - \frac{1}{2\pi^2} \sum_{l=e,\mu,\nu_e,\nu_\mu} g_l \int_0^\infty dk \, k^2 \left((1 - f(k, m_l, \mu_l)) \ln(1 - f(k, m_l, \mu_l)) \right) \\ - \frac{1}{2\pi^2} \sum_{l=e,\mu,\nu_e,\nu_\mu} g_l \int_0^\infty dk \, k^2 \left((1 - f_a(k, m_l, \mu_l)) \ln(1 - f_a(k, m_l, \mu_l)) \right) \end{aligned} \quad (34)$$

For numerical calculation of thermodynamic characteristics of hadronic matter, the following values of RMF model parameters were used: $a_\sigma = 9.154$ fm^2, $a_\omega = 4.828$ fm^2, $a_\delta = 2.5$ fm^2, $a_\rho = 13.621$

fm^2, $b = 1.654\ 10^{-2}$ fm^{-1}, $c = 1.319\ 10^{-2}$ [24]. These values were obtained based on the requirement of an acceptable description of such well-known nuclear parameters as: bare nucleon mass $m_N = 938.93$ MeV, nuclear matter saturation density $n_0 = 0.153$ fm^{-3}, nucleon effective mass at saturation density $m_N^* = 0.78\ m_N$, nuclear matter compressibility modulus $K = 300$ MeV, binding energy per nucleon $f = -16.3$ MeV, symmetry energy $E_{sym}^{(0)} = 32.5$ MeV.

2.3. Deconfinement Phase Transition in Presence of Trapped Neutrinos

To construct the hybrid equation of state for hot and dense strongly interacting matter, it is not sufficient to know the separate equations of state for hadronic and quark matter. It is also very important to know what kind of phase transition from hadronic matter to quark matter is. In the case of phase transitions of atomic-structured matter, there is one conserved quantity, namely the number of atoms. The phase transition occurs according to Maxwell's construction. Phase coexistence occurs at a specific pressure P_0, while other thermodynamic quantities, such as energy density and baryon number density, change abruptly. In contrast, in the phase transition from hadronic matter to quark matter, there are two conserved quantities: baryon number and electric charge.

As shown in Ref.[55], in the case of more than one conserved quantity, the Gibbs equilibrium condition between phases allows for a phase transition in which the thermodynamic parameters change continuously. The coexistence between phases in this case occurs not at a single pressure value P_0, but in a continuously changing range, starting from the pressure value P_H to the pressure value P_Q, during which the volume fraction of the quark phase in the mixed phase increases from zero to one. In Maxwell's construction, the assumption is made that the condition of local electrical neutrality applies, meaning that each of the two phases is electrically neutral on its own. In contrast, Gibbs construction relies on the principle of global electroneutrality, where the two phases can have separate charges but still ensure that the overall system remains electrically neutral.

Which of the two phase transition scenarios described here is energetically more preferable depends on the value of the surface tension at the interface between the quark phase and hadronic phase. Currently, there are no reliable data on the surface tension of the hadron-quark interface. Theoretical estimates are model-dependent and predict a range of values from a few MeV/fm^2 to hundreds of MeV/fm^2 [56–63]. This uncertainty in the surface tension coefficient at the hadron-quark interface does not allow for unambiguous conclusions as to which scenario of phase transition is occurring.

In this work, we have assumed that the surface tension is so strong that the formation of a mixed phase is not energetically favorable, so that the transition from hadronic matter to quark matter will be a normal first-order phase transition determined by the Maxwellian construction.

The thermodynamic description of quark matter presented in Subsection 2.1 allows us to numerically determine the dependence of pressure on temperature and baryon number density, $P_{QM}(T, n_B)$. Similarly, the dependence of the baryon chemical potential on the temperature and baryon density is also determined: $\mu_B(T, n_B)$. As a result, we have the dependence $P_{QM}(T, \mu_B)$. In the same way, within the framework of the model described in Subsection 2.2, the dependence $P_{HM}(T, \mu_B)$ of hadronic matter is numerically determined.

The baryon chemical potentials in the hadronic and quark phases are determined as follows:

$$\mu_B{}^{HM} = \mu_n, \quad \mu_B{}^{QM} = \mu_u + 2\mu_d. \tag{35}$$

The characteristics of the first-order phase transition at a given temperature are determined according to Maxwell's construction:

$$P_{HM}(T, \mu_B) = P_{QM}(T, \mu_B) = P_0(T), \quad \mu_B{}^{HM} = \mu_B{}^{QM} = \mu_{B0}(T). \tag{36}$$

Knowing the phase transition pressure P_0 and the baryon chemical potential μ_{B0} in the phase coexistence state allows you to determine the other characteristics of the transition, such as: the baryon

Preprints.org (www.preprints.org) | NOT PEER-REVIEWED | Posted: 9 March 2026 doi:10.20944/preprints202603.0555.v1

number densities of coexistence n_H and n_Q, as well as the energy densities ε_H and ε_Q, and the entropy densities S_H and S_Q in coexistence.

3. Numerical Results and Discussion

Within the framework of the models described above, we calculated the thermodynamic characteristics of beta-equilibrated, electrically neutral hadronic matter and three-flavor quark matter. Based on these results, we determined the parameters for the Maxwellian phase transition at different temperatures. The calculations were conducted under two conditions: one where neutrinos are trapped, and another where neutrinos have already left the stellar matter.

The left panel of Figure 1 illustrates how the masses of constituent quarks depend on baryon number density at a temperature of $T = 50$ MeV, both in the presence of neutrinos and in their absence. Notably, at high densities, the presence of neutrinos significantly influences the mass of the strange quark, while having minimal impact on the masses of the light quarks. In the region of high baryon number density, the presence of neutrinos causes an increase in the mass of the s quark, whereas the masses of the u and d quarks experience a slight decrease.

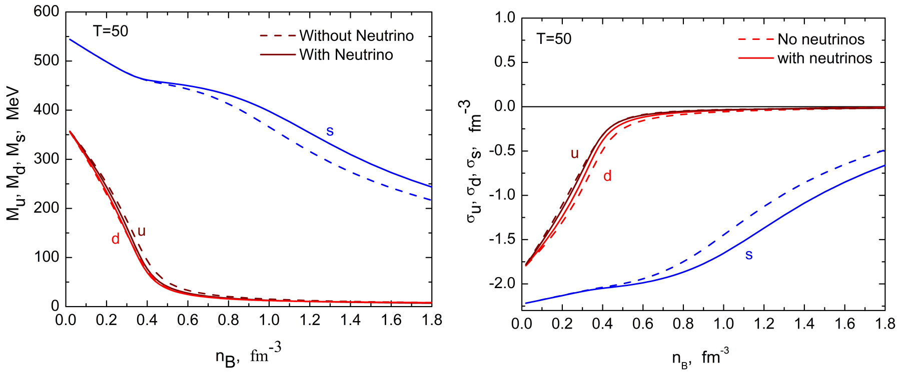

(**a**) (**b**)

Figure 1. (**a**) Constituent quark masses M_u, M_d, and M_s as a function of the baryon number density n_B at temperature $T = 50$ MeV. (**b**) Quark condensates σ_u, σ_d, and σ_s as a function of the baryon number density n_B at temperature $T = 50$ MeV. Solid lines correspond to the neutrino-trapped regime, and dashed lines to the neutrino-transparent regime.

The effect of neutrinos on quark condensates σ_u, σ_d, and σ_s, which mediate the strong interaction between quarks of different flavors within the Nambu–Jona-Lasinio (NJL) model and lead to the dynamic generation of quark masses, is illustrated in the right panel of Figure 1. As we can observe, the presence of neutrinos in the high baryon number density region significantly impacts the condensate σ_s, which has a negative value and decreases (meaning it increases in absolute value). Meanwhile, the change in σ_u is negligible, while σ_d experiences a slight increase (meaning it decreases in absolute value).

Figure 2 illustrates the relationship between energy per baryon $E_1 = \varepsilon/n_B$ and baryon number density n_B for quark matter in β-equilibrium at temperatures of $T = 20$ MeV and $T = 100$ MeV. The presence of neutrinos results in an increase in energy per baryon at a given baryon number density. At lower temperatures, there exists a number density value that corresponds to the minimum energy per baryon. However, as the temperature rises, this minimum disappears in matter without neutrinos. In the neutrino-trapped regime, the minimum of energy per baryon shifts to higher densities with increasing temperature but does not disappear.

 doi:10.20944/preprints202603.0555.v1

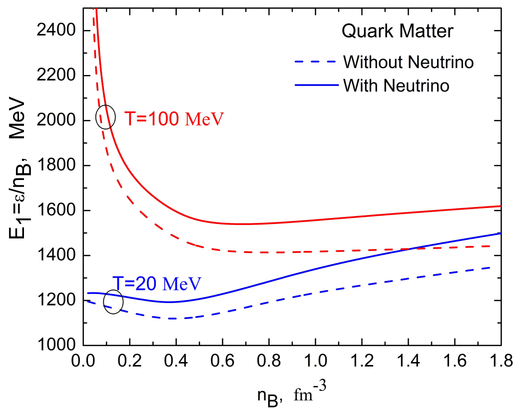

Figure 2. Energy per baryon E_1 as a function of the baryon number density n_B at $T = 20$ MeV and $T = 100$ MeV. Solid lines correspond to the neutrino-trapped regime, and dashed lines to the neutrino-transparent regime.

Figure 3 shows the dependence of pressure P on the baryon number density n_B (panel a), as well as on the energy density ε (panel b) for two temperatures: $T = 20$ MeV and $T = 100$ MeV. The pressure at a given baryon number density n_B is higher in the presence of trapped neutrinos than in its absence. A similar trend is observed in the dependence on energy density ε. In contrast to the previous case, the increase in pressure at a given energy density with increasing temperature becomes less noticeable.

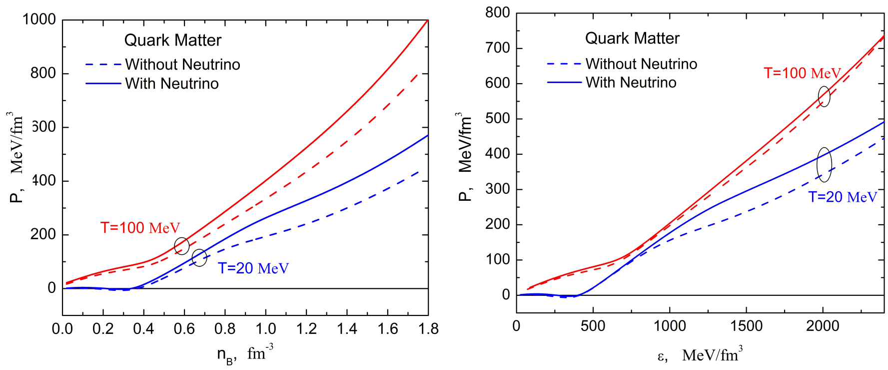

(**a**) (**b**)

Figure 3. (**a**) Pressure P of strange quark matter as a function of the baryon number density n_B at $T = 20$ MeV and $T = 100$ MeV. (**b**) Pressure P of strange quark matter as a function of the energy density ε at $T = 20$ MeV and $T = 100$ MeV. Solid lines correspond to the neutrino-trapped regime, and dashed lines to the neutrino-transparent regime.

The dependences of the baryon chemical potential μ_B and baryon number density n_B on pressure P for both quark matter and hadronic matter at temperatures $T = 0$ MeV, $T = 50$ MeV, $T = 74$ MeV, and $T = 75$ MeV are shown in Figure 4. The intersection of the curves in the $\mu_B - P$ plane determines the first-order phase transition parameters, such as the phase equilibrium pressure P_0 and μ_{B_0}. Knowing the phase equilibrium pressure P_0 allows us to find the baryon number densities n_H and n_Q corresponding to phase equilibrium using a graph of the baryon number density n_B as a function of pressure P. Figure 4(**a**) shows the case of cold matter in which there are no neutrinos.

 doi:10.20944/preprints202603.0555.v1

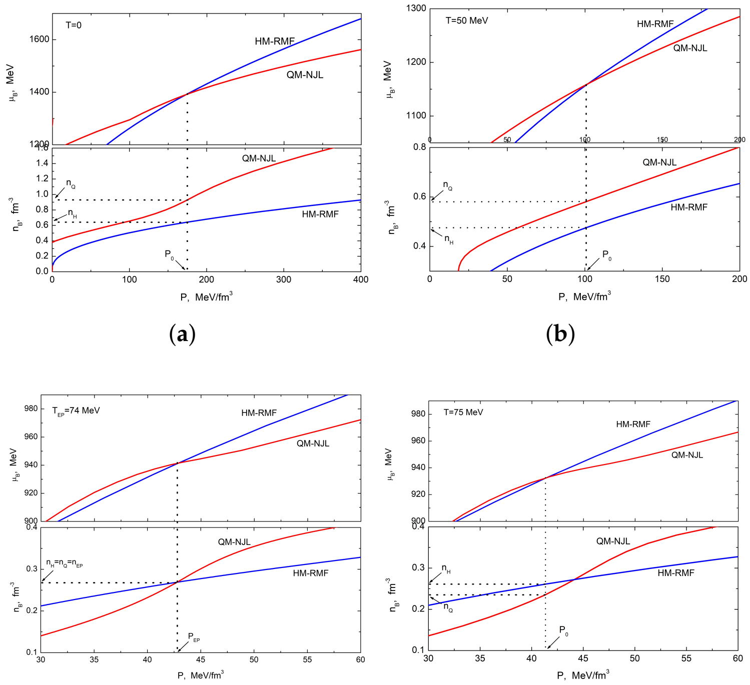

(a) (b) (c) (d)

Figure 4. The baryon chemical potential μ_B and baryon number density n_B are plotted as functions of pressure P for both quark matter and hadronic matter at various temperatures: (**a**) $T = 0$ MeV; (**b**) $T = 50$ MeV; (**c**) $T = 74$ MeV; and (**d**) $T = 75$ MeV. The dotted lines indicate the parameter values corresponding to the coexistence of the two phases.

With increasing temperature, the baryon number densities n_H and n_Q, corresponding to the state of equilibrium coexistence of the hadron and quark phases, decrease. At relatively low temperatures, the density of quark matter at equilibrium, n_Q, is greater than the corresponding density n_H of hadronic matter. At a certain temperature T_{cr}, the baryon number densities of both phases are equal: $n_H(T_{cr}) = n_Q(T_{cr}) = n_{cr}$ (Panel (**c**)). At temperatures above this critical temperature, the condition $n_Q < n_H$ is satisfied (see Panel (**d**)). In this temperature range, the phase transition ceases to be a first-order transition; it acquires the character of a crossover. In the model we are considering, the parameters of the critical endpoint for matter in the neutrino trapping regime are as follows: $n_{cr} = 0.269$ fm^{-3} and $T_{cr} = 74$ MeV.

In Table 1, we present the coexistence parameters of the hadronic phase and quark phase for stellar neutrino-trapped matter at different temperatures. The first line shows the phase transition parameters for cold neutrino-free matter. The last line presents the characteristic parameters of the critical endpoint in the neutrino-trapped regime, when the baryon number densities of both phases in the coexistence state become equal.

The numerical calculation results of the parameters for the equilibrium state of coexistence between the quark and hadron phases at various temperatures in the neutrino-transparent regime are presented in Table 2. When we compare the results from the neutrino trapping regime to those from the neutrino-transparent regime, we observe that, at a given temperature, the presence of neutrinos increases the phase equilibrium pressure P_0. Concurrently, it decreases the equilibrium chemical potential μ_{B0}. The presence of neutrinos at a given temperature decreases the baryon number density of the quark phase, n_Q, in the phase coexisting state. However, the baryon number density of the hadron phase in the phase coexistence state n_H does not change consistently; it increases at low temperatures and decreases at high temperatures. The presence of neutrinos leads to an increase in the entropy per baryon S_H/n_H and S_Q/n_Q for both phases in a state of phase equilibrium.

 doi:10.20944/preprints202603.0555.v1

Table 1. First-order deconfinement phase transition parameters for hot and dense stellar neutrino-trapped matter. ϵ_H and ϵ_Q represent the phase equilibrium energy densities for the hadron and quark phases, respectively, while S_H/n_H and S_Q/n_Q denote the entropy per baryon for these phases in their coexistence state.

T MeV	P_0 MeV/fm^3	μ_B MeV	n_H fm^{-3}	n_Q fm^{-3}	ε_H MeV/fm^3	ε_Q MeV/fm^3	S_H/n_H fm^{-3}	S_Q/n_Q fm^{-3}
0	173.6	1391.8	0.639	0.918	716.3	1109.2	0	0
5	198.7	1377.9	0.683	0.829	795.9	1058.7	0.154	0.346
10	194.8	1370.5	0.676	0.821	787.1	1049.8	0.307	0.683
20	181.3	1343.8	0.652	0.792	756.1	1015.0	0.601	1.322
30	159.2	1298.4	0.609	0.738	703.4	950.1	0.865	1.858
50	101.9	1160.2	0.478	0.583	547.0	766.3	1.232	2.509
70	46.2	966.9	0.290	0.371	336.4	522.2	1.253	2.541
72	44.1	953.1	0.278	0.325	324.6	467.4	1.251	2.442
74	42.7	941.2	**0.269**	**0.269**	315.6	397.2	1.261	2.275

Table 2. First-order deconfinement phase transition parameters for hot and dense stellar neutrino-free matter.

T MeV	P_0 MeV/fm^3	μ_B MeV	n_H fm^{-3}	n_Q fm^{-3}	ε_H MeV/fm^3	ε_Q MeV/fm^3	S_H/n_H fm^{-3}	S_Q/n_Q fm^{-3}
0	173.6	1391.8	0.639	0.918	716.3	1109.3	0	0
5	172.2	1389.3	0.637	0.914	713.2	1098.9	0.148	0.355
20	159.6	1360.2	0.611	0.847	683.2	1018.5	0.570	1.313
30	143.6	1320.6	0.576	0.784	642.6	945.6	0.784	1.792
50	97.5	1195.5	0.469	0.629	520.0	773.5	1.134	2.372
70	50.7	1016.2	0.318	0.448	356.0	580.6	1.187	2.515
75	39.7	959.0	0.290	0.344	304.5	465.0	1.137	2.329
75.6	36.0	942.4	**0.255**	**0.255**	288.0	357.6	1.106	2.027

Figure 5 illustrates the particle number densities as a function of baryon number density n_B for stellar matter, considering a first-order phase transition at four different temperatures. Panel (**a**) displays these relationships for cold matter, where neutrinos are not present. In this scenario, the quark phase features a reduced electron count, muons are absent, and the quark component is primarily responsible for maintaining electrical neutrality.

Panel (**b**) shows particle populations at a relatively low temperature of $T = 10$ MeV. The presence of neutrinos significantly reduces the number of muons while increasing the number of electrons in the hadron phase. Protons and electrons are crucial for maintaining electrical neutrality in this phase. Additionally, neutrinos contribute to a higher number of electrons in the quark phase, making electrons important for preserving electrical neutrality in that phase as well.

From Figure 5, it is clear that as the temperature increases, the magnitude of the abrupt change in baryon number density during the first-order phase transition—illustrated as a grey rectangular region - decreases. Notably, at a temperature of $T_{cr} = 74$ MeV, this jump in baryon number density disappears completely. At sufficiently high temperatures in the region of high baryon densities, the presence of μ^+ with the corresponding neutrino ν_μ becomes energetically favorable compared to the pair μ^- and $\tilde{\nu}_\mu$.

In the hadron phase, neutrons are the most abundant particles. In the quark phase, the down (d) quark is the most prevalent particle in regions of baryon number density where the negative muon (μ^-) is energetically favorable. However, above the production threshold for positive muons (μ^+), the up (u) quark becomes the most abundant.

 doi:10.20944/preprints202603.0555.v1

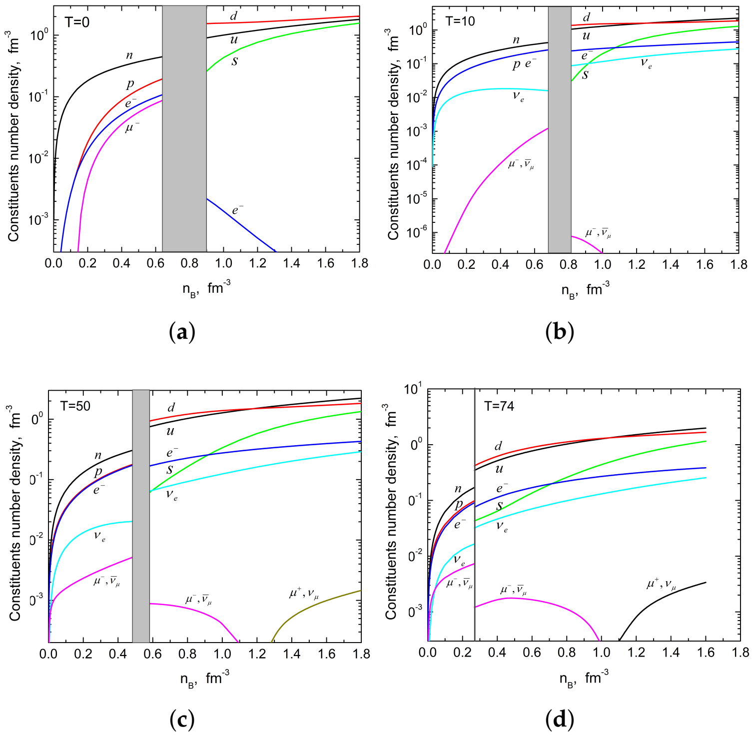

Figure 5. Number densities of constituents as a function of baryon number density n_B, considering a first-order phase transition at different temperatures: (**a**) $T = 0$ MeV; (**b**) $T = 10$ MeV; (**c**) $T = 50$ MeV; and (**d**) $T = 74$ MeV. The grey rectangular regions correspond to the abrupt change in the baryon number density during an ordinary first-order phase transition in accordance with Maxwell's construction.

Figure 6 illustrates the phase diagram for the deconfinement phase transition within the model we considered. Panel (a) displays the boundary lines of the first-order phase transition in the temperature-baryon chemical potential ($T - \mu_B$) plane. The solid line represents the neutrino-trapped regime, while the dashed line indicates the neutrino-free regime. As we can see, the presence of neutrinos reduces the baryon chemical potential during phase coexistence at the same temperature. The circles show the corresponding critical endpoints at which the baryon number densities of the coexistence of the quark and hadron phases become equal. The parameters corresponding to the critical endpoint in the neutrino-trapped regime are detailed in the last row of Table 1. Similarly, the last row of Table 2 exhibits comparable characteristics for neutrino-free matter. The presence of neutrinos leads to a decrease in the critical temperature from 75.6 MeV to 74 MeV, while the critical baryon chemical potential also decreases from 942.4 MeV to 941.2 MeV.

Panel (b) of Figure 6 represents the phase diagram in the $T - n_B$ plane. The solid blue line corresponds to the hadron phase in equilibrium with the quark phase in the neutrino-trapped regime, and the dashed blue line corresponds to the hadron phase in equilibrium with the quark phase in the neutrino-free regime. Analogous red lines correspond to the quark phase in equilibrium with the hadron phase. The presence of neutrinos leads, at a given temperature, to a decrease in the baryon number density of quark matter in phase equilibrium with hadronic matter. Regarding hadronic matter, the effect of neutrinos on the baryon number density of hadronic matter in phase equilibrium with quark matter varies across different temperature ranges. At $T < 54.4$ MeV, the presence of neutrinos at a given temperature increases the baryon number density of hadronic matter in phase equilibrium with quark matter. At 54.4 MeV$< T < T_{cr}$, conversely, it leads to a decrease in the baryon number density of hadronic matter at the phase transition point.

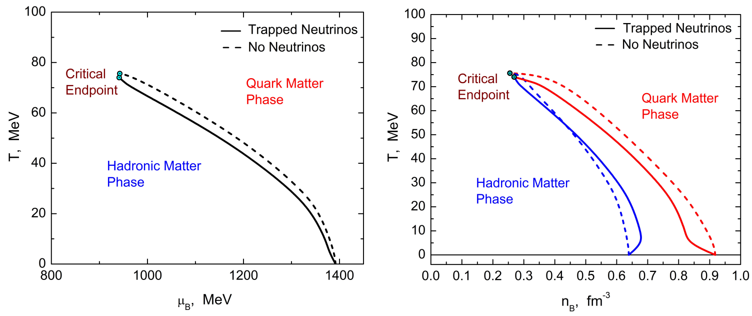

(a) (b)

Figure 6. Phase diagrams for stellar matter with a first-order deconfinement phase transition within the RMF-NJL model used in this paper: (**a**) Phase diagram $T - \mu_B$. The solid line indicates the coexistence of hadronic and quark phases in the neutrino-trapping regime, while the dashed line indicates the coexistence of hadronic and quark phases in the neutrino-transparent regime. (**b**) Phase diagram $T - n_B$. The solid blue line indicates the boundary of the hadronic matter region within the neutrino-trapping regime, while the solid red line represents the boundary of the quark matter region in the same regime. The dashed blue line denotes hadronic matter in the neutrino-transparent regime, and the dashed red line represents quark matter in a similar regime.

4. Conclusions

In this study, we investigated how trapped neutrinos affect the properties of the quark deconfinement phase transition in hot β-equilibrated electrically neutral hadronic matter. To describe the thermodynamic properties of hot hadronic stellar matter, we utilized the relativistic mean-field theory, which also incorporated the isovector–Lorentz-scalar δ-meson effective field. We used the local SU(3) NJL model to describe the three-flavor quark phase.

The thermodynamic properties of the quark and hadronic phases, in both the neutrino-trapped and neutrino-transparent regimes, have been calculated for various temperature and baryon number density values. It has been shown that at high baryon number densities, the presence of neutrinos leads to a significant increase in the constituent mass of the s quark, while the masses of the u and d quarks experience a slight decrease. The presence of neutrinos also leads to similar changes in the absolute values of quark condensates σ_u, σ_d, and σ_s, which dictate the strong interaction among quarks of different flavors.

Our study indicates that in the neutrino-trapping regime, the energy per baryon of quark matter is higher for a given baryon density compared to the neutrino-transparent regime. In the temperature range considered, the pressure of quark matter with neutrinos present at the same baryon number density is significantly higher than in their absence. Additionally, the presence of neutrinos contributes to an increase in energy density; however, this increase becomes quite minimal as the temperature rises.

The effect of trapped neutrinos on the thermodynamic characteristics of the coexistence of quark matter and hadronic matter has been studied. It has been shown that the baryon chemical potential of the coexistence state decreases with increasing temperature. The corresponding baryon number densities of phases n_H, n_Q also decrease. At some temperature T_{cr}, the baryon densities of the coexistence state of the two phases become equal to each other. At temperatures higher than this temperature, the density of hadronic matter in the coexistence state exceeds the density of quark matter. The temperature of T_{cr} is the critical endpoint of the first-order deconfinement phase transition, above which we deal with a crossover transition. Within the framework of the model we used, the temperature corresponding to the critical endpoint was found to be 74 MeV in the neutrino-trapping regime, and 75.6 MeV in the neutrino-transparent regime.

By examining the alterations in the phase diagram in the $T - n_B$ plane caused by the presence of trapped neutrinos, we have concluded that at a given temperature, neutrinos decrease the baryon number density n_Q of quark matter in phase equilibrium with hadronic matter. The effect of neutrinos on the baryon number density of hadronic matter in phase equilibrium with quark matter varies across different temperature ranges. At temperatures below 54.4 MeV, the presence of neutrinos increases the baryon number density n_H of hadronic matter in equilibrium with quark matter. However, in the temperature range of 54.4 MeV to the critical temperature T_{cr}, neutrinos cause a decrease in the baryon number density n_H of hadronic matter in a coexistence state of two phases.

In this article, we have not taken into account the neutrino flavor changes, also known as neutrino oscillations. The effects of incorporating neutrino oscillations will be the focus of a separate study that we plan to conduct in the near future.

References

1. Collins, J. C.; Perry, M.J. Superdense matter: neutrons or asymptotically free quarks?. *Phys. Rev. Lett.* **1975**, 34, 1353–1356.
2. Karsch, F. The phase transition to the quark gluon plasma: recent results from lattice calculations. *Nucl. Phys. A* **1995**, 590, 367–381.
3. STAR Collaboration.; Adams, J.; Aggarwal, M. M.; Ahammedet, Z.; et al. Experimental and theoretical challenges in the search for the quark gluon plasma: the STAR Collaboration's critical assessment of the evidence from RHIC collisions. *Nucl. Phys. A* **2005**, 757, 102–183.
4. Busza, W.; Rajagopal, K.; van der Schee W. Heavy ion collisions: the big picture, and the big questions. *Ann. Rev. Nucl. Part. Sci.* **2018**, 68, 339–376.
5. Nagamiya S. Heavy-Ion Collisions toward High-Density Nuclear Matter. *Entropy* **2022**, 24, 482.
6. ALICE Collaboration.; Acharya, S.; Adamová, D.; Adler, A; et al. The ALICE experiment: a journey through QCD. *Eur. Phys. J. C* **2024**, 84, 813.
7. CMS Collaboration; Hayrapetyan, A.; Aarrestad, T. K.; Androsov, K.; et al. Overview of high-density QCD studies with the CMS experiment at the LHC. *Phys. Rep.* **2025**, 1115, 219–367.
8. Lu, Y.;Gao, F.; Luo, X .; Chang, L.; Liu, Y. Revealing the signal of QCD phase transition in heavy-ion collisions. *Sci. China Phys. Mech. Astron.* **2025** 68, 251012.
9. Kumar, R.; Dexheimer, V.; Jahan, J.; et al. Theoretical and experimental constraints for the equation of state of dense and hot matter. *Living Reviews in Relativity* **2024**, 27, 3 (115 p.).
10. Elfner, H.; Müller,B. The exploration of hot and dense nuclear matter: introduction to relativistic heavy-ion physics. *J. Phys. G: Nucl. Part. Phys.* **2023**, 50 103001.
11. Shapiro, S. L.; Teukolsky, S. A. 1983. *Black Holes, White Dwarfs, and Neutron Stars: The Physics of Compact Objects*. Publication place: John Wiley & Sons, New York.
12. Glendenning, N. 2000. *Compact Stars: Nuclear Physics, Particle Physics, and General Relativity*. Publication place: Springer, Berlin.
13. Lattimer, J.M.; Prakash, M.The physics of neutron stars. *Science* **2004**, 304, 536—542.
14. Weber, F.; Negreiros, R.; Rosenfield, P.; Stejner, M. Pulsars as astrophysical laboratories for nuclear and particle physics. *Prog. Part. Nucl. Phys.* **2007**, 59, 94—113.
15. Riley, T. E.; Watts, A. L.; Bogdanov, S.; et al. A NICER View of PSR J0030+0451: Millisecond Pulsar Parameter Estimation. *ApJL* **2019**, 887, L21.
16. Miller, M. C.; Lamb, F. K.; Dittmann, A. J.; et al.PSR J0030+0451 Mass and Radius from NICER Data and Implications for the Properties of Neutron Star Matter. *ApJL* **2019**, 887, L24.
17. Salmi, T.; Vinciguerra, S.; Choudhury, D.; et al. The Radius of PSR J0740+6620 from NICER with NICER Background Estimates. *ApJ* **2022**, 941, 150.
18. Chodos, A.; Jaffe, R. L.; Johnson, K.; Thorn, C. B.; Weisskopf, V.F. New extended model of hadrons. *Phys. Rev. D* **1974**, 9, 3471–3495.
19. Schertler, K.; Greiner, C.; Schaffner-Bielich, J.; Thoma, M.H. Quark phases in neutron stars and a third family of compact stars as signature for phase transitions. *Nucl. Phys. A* **2000**, 677, 463–490.
20. Alaverdyan, G. B.; Harutyunyan, A. R.; Vartanyan, Y. L. Low-mass quark stars or quark white dwarfs. *Astrophysics* **2001**, 44, 265-–275.
21. Burgio, G. F.; Baldo, M.; Sahu, P. K.; Schulze, H. -J. Hadron-quark phase transition in dense matter and neutron stars. *Phys. Rev. C* **2002**, 66, 025802.
22. Alaverdyan, G. B.; Harutyunyan, A. R.; Vartanyan, Y. L. Neutron stars with a quark core. II. basic integral and structural parameters. *Astrophysics* **2004**, 47, 52—64.
23. Sharma, B. K.; Panda, P. K.; Patra, S. K. Phase transition and properties of a compact star. *Phys. Rev. C* **2007**, 75, 035808.

24. Alaverdyan, G. B. Relativistic mean-field theory equation of state of neutron star matter and a Maxwellian phase transition to strange quark matter. *Astrophysics* **2009**, 52, 132–150.
25. Alaverdyan, G. B. Influence of a Scalar-isovector δ-meson field on the quark phase structure in neutron stars. *Res. Astron. Astrophys.* **2010**, 10, 1255-–1264.
26. Negreiros, R.; Dexheimer, V. A.; Schramm, S. Quark core impact on hybrid star cooling. *Phys. Rev. C* **2012**, 85, 035805.
27. Alaverdyan, G. B.; Vartanyan, Y. L. Maximum mass of hybrid stars in the quark bag model. *Astrophysics* **2017**, 60, 563—571
28. Perego, A.; Bernuzzi, S.; Radice, D. Thermodynamics conditions of matter in neutron star mergers. *Eur. Phys. J. A* **2019**, 55, 124.
29. Hajyan, G.; Alaverdyan, A. Hot Strange Stars. I. Equation of State of Hot Strange Quark Matter. *Astrophysics* **2014**, 57, 559–569.
30. Cardoso, P. H. G.; Nunes da Silva, T.; Deppman, A; Menezes, D. P. Quark matter revisited with non-extensive MIT bag model. *Eur. Phys. J. A* **2017**, 53, 191.
31. Hajyan, G. S. Characteristics of Hot Quark Matter with Neutrino Confinement. *Astrophysics* **2020**, 63, 125–132.
32. Xu, S. -S. Phase structures of neutral dense quark matter and application to strange star. *Chinese Phys. C* **2022**, 46, 014105.
33. Pal, S.; Chaudhuri G. Medium effects in the MIT bag model for quark matter: Self-consistent thermodynamical treatment. *Phys. Rev. D* **2023**, 108, 103028
34. Podder, S.; Pal, S.; Sen, D.; Chaudhuri, G. Constraints on density dependent MIT bag model parameters for quark and hybrid stars, *Nuclear Physics A* **2024**, 1042, 122796.
35. Nambu, Y.; Jona-Lasinio, G. Dynamical Model of Elementary Particles Based on an Analogy with Superconductivity. I. *Phys. Rev.* **1961**, 122, 345–358.
36. Nambu, Y.; Jona-Lasinio, G. Dynamical Model of Elementary Particles Based on an Analogy with Superconductivity. II. *Phys. Rev.* **1961**, 124, 246–254.
37. Rehberg, P.; Klevansky, S.P.; Hüfner, J. Hadronization in the SU (3) Nambu–Jona-Lasinio model. *Phys. Rev. C* **1996**, 53, 410–429.
38. Buballa, M. NJL–model analysis of dense quark matter. *Phys. Rep.* **2005**, 407, 205–375.
39. Volkov, M.K.; Radzhabov, A.E. The Nambu–Jona-Lasinio model and its development. *Phys. Uspekhi* **2006**, 49, 551–562.
40. Bonanno, L.; Sedrakian, A. Composition and stability of hybrid stars with hyperons and quark color-superconductivity. *A&A* **2012**, 539, A16.
41. Ranea-Sandoval, I. F.; Orsaria, M. G.; Han, S.; Weber, F.; Spinella, W. M. Color superconductivity in compact stellar hybrid configurations. *Phys. Rev. C* **2017**, 96, 065807.
42. Alaverdyan, G.B. Vartanyan, Y.L. Hybrid Stars in the Framework of the Local Nambu-Jona-Lasinio Model for Quark Matter. *Astrophysics* **2018**, 61, 483–498.
43. Alaverdyan, G. Hadron–Quark Phase Transition in the SU (3) Local Nambu–Jona-Lasinio (NJL) Model with Vector Interaction. *Symmetry* **2021**, 13, 124.
44. Contrera, G. A.; Blaschke, D.; Carlomagno, J. P. Quark-nuclear hybrid equation of state for neutron stars under modern observational constraints. *Phys. Rev. C* **2022**, 105, 045808.
45. Yuan, W.-L.; Gao, B.; Yan, Y.; Xu, R. Hybrid stars with large quark cores within the parity doublet model and modified NJL model. *Phys. Rev. D* **2025**, 112, 023019.
46. Serot, B.D.; Walecka, J.D.The Relativistic nuclear many-body problem. *Adv. Nucl. Phys.* **1986**, 16, 1–327.
47. Serot, B.D.; Walecka, J.D. Recent progress in quantum hadrodynamics. *Int. J. of Mod. Phys. E* **1997**, 6, 515–631.
48. Alaverdyan, G.B., Alaverdyan, A.G. Isospin-Asymmetric Cold Nuclear Matter in the Relativistic Mean-Field Theory with a Scalar-Isovector Interaction Channel. *Astrophysics* **2024**, 67, 215–230.
49. Alaverdyan, G.B.; Hajyan, G.S.; Alaverdyan, A.G. Numerical Modeling of Thermodynamic Parameters for Hot Neutron Star Matter in Neutrino-Trapped Regime. *Phys. Part. Nuclei* **2025** 56, 1318–1322.
50. Hajyan, G.S., Alaverdyan, G.B. Hot Quark Matter with Neutrino Confinement in Terms of the Local Nambu – Jona-Lasinio SU(3) Model. *Astrophysics* **2021**, 64, 370–387.
51. Prakash, M.; Bombaci, I.; Prakash, M.; Ellis, P.J.; Lattimer, J. M.; Knorren, R. Composition and structure of protoneutron stars. *Phys. Rep.*1997 **280**,1–77.
52. Roark, J.; Dexheimer, V. Deconfinement phase transition in proto-neutron-star matter. *Phys. Rev. C* **2018**, *98*, 055805.

 doi:10.20944/preprints202603.0555.v1

53. Xia, C.-J.; Maruyama, T.; Yasutake, N.; Tatsumi, T. Constraining quark-hadron interface tension in the multimessenger era. *Phys. Rev. D* **2019**, *99*, 103017.
54. Malfatti, M.; Orsaria, M.G.; Contrera, G.A.; Weber, F.; Ranea-Sandoval, I.F. Hot quark matter and (proto-) neutron stars. *Phys. Rev. C* **2019** *100*, 015803.
55. Glendenning, N. K. First-order phase transitions with more than one conserved charge: Consequences for neutron stars. *Phys. Rev. D* **1992**, 46, 1274–1287.
56. Alford, M.; Rajagopal, K.; Reddy, S.; Wilczek, F. Minimal color-flavor-locked–nuclear interface. *Phys. Rev. D* **2001**, 64, 074017.
57. Wen, X. J.; Li, J. Y.; Liang, J. Q.; Peng, G. X. Medium effects on the surface tension of strangelets in the extended quasiparticle model. *Phys. Rev. C* **2010**, 82, 025809.
58. Lugones, G.; Grunfeld, A. G.; Ajmi, M. A. Surface tension and curvature energy of quark matter in the Nambu–Jona-Lasinio model. *Phys. Rev. C* **2013**, 88, 045803.
59. Gao, F.; Liu, Y. Interface effect in QCD phase transitions via Dyson-Schwinger equation approach. *Phys. Rev. D* **2016**, 94, 094030.
60. Xia, C.-J.; Peng, G.-X.; Sun, T.-T.; Guo, W.-L.; Lu, D.-H.; Jaikumar, P. Interface effects of strange quark matter with density dependent quark masses. *Phys. Rev. D* **2018**, 98, 034031.
61. Fraga, E.S.; Hippert, M.; Schmitt, A. Surface tension of dense matter at the chiral phase transition. *Phys. Rev. D* **2019**, 014046.
62. Lugones, G.; Grunfeld, A. G. Surface tension of hot and dense quark matter under strong magnetic fields. *Phys. Rev. C* **2019**, 99, 035804
63. Constantinou, C.; Guerrini, M.; Zhao, T.; Han, S.; Prakash, M. Framework for phase transitions between the Maxwell and Gibbs constructions at finite temperature. *Phys. Rev. D* **2025**, 112, 094014.